EFFECT OF CASE-HARDENING ON CONTACT FATIGUE AND WEAR DAMAGE OF ASTALOY CRM BASED PM STEEL

D. Rodziňák, R. Zahradníček, P. Hvizdoš, K. Semrád, D. Jakubéczyová

Abstract

The paper deals with contact fatigue properties of a PM material based on a sintered iron powder of Astaloy CrM type with 0.3% C with a density of 7 g·cm^{-3}. The investigation was focused on the effect of case-hardening using samples with and without surface toughening treatment by shoot peening. Case-hardening increased the fatigue limit at 50·10^6 cycles by 36%, the achieved value is as high as 1790 MPa, when compared to as sintered state. The beneficial effect of the shoot penning of the surface increased the fatigue limit at 50·10^6 cycles by 63%, before case-hardening and reached the value 2920 MPa. The samples after the contact fatigue testing were examined by metallographic microscopic observation. Wear damage was also studied by the pin-on-disc technique. It has been found that this type of material behaves in specific ways depending on the surface layers properties after the mentioned treatment.

Keywords: Cr–sintered steels, contact fatigue, wear, surface modification

INTRODUCTION

Astaloy CrM type powder is a commercial PM material produced by Höganäs AB and is, similarly to Astaloy CrL powder, designed for the manufacturing of machine parts for demanding applications such as cog wheels or roller bearings. During their time in service they are exposed to both contact fatigue and wear. For their practical utilization and reliable functioning, it is necessary to know their resistance against these types of contact loading as well as to understand factors that affect this resistance. Currently, great worldwide attention is given to both mentioned powders and their properties following various types of processing, as described in [1-10].

EXPERIMENTAL

The experimental material the iron powder of CrM type (Fe–3Cr-0.5Mo) manufactured by Höganäs AB was used. From it, with the addition of 0.3% C and 0.5% of HW lubricant, disc samples with dimensions of ∅ 30 x 5 mm were die-pressed using 600 MPa pressure. These were sintered at 1120°C/60 min in 90% N_2 + 10% H_2 atmosphere. In order to prevent oxidation, the atmosphere (dew point -57°C) had been cooled down and the samples were stored in a retort in Al_2O_3 + 5% C powder bed. After sintering, the cooling was done outside the furnace in a retort with protective atmosphere. The samples produced were mechanically machined to ∅ 28 mm with a central opening of ∅ 10 mm. Some of the samples

Dušan Rodziňák, Rudolf Zahradníček, Karol Semrád, Faculty of Aeronautics, Technical University of Košice, Košice, Slovak Republic
Pavol Hvizdoš, Dagmar Jakubéczyová, Institute of Materials Research, Slovak Academy of Sciences, Košice, Slovak Republic

were treated by shoot peening from both sides by steel granulate with the size ∅ 0.6 mm at 7000 rpm. The angle of shoot peening was 90° and 9 kg of steel granulate was used for both sides.

Subsequently, the samples were case-hardened at 900°C for 3 hours. The case-hardening environment charcoal with an addition of 5% $BaCO_3$ was used. After that, the temperature was lowered to 850°C and from this temperature the samples were hardened by being dropped into oil. After hardening they were tempered for 60 min at 180°C.

The samples were subjected to standard hardness testing, metallographic analysis and contact fatigue tests using the AXMAT equipment (Fig.1a). The frequency used was about 500 cycles per second. Transmission oil Mogul SAE 80 was used as lubricant.

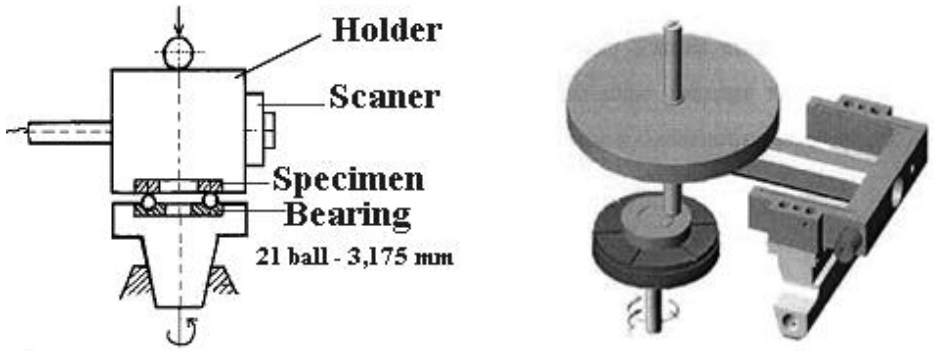

Fig.1a, b. Principles of the – AXMAT and CSM testing equipment.

Tribological testing was carried out on a CSM Tribometer, the principle of which is illustrated in Fig.1b. All measurements were tested under the same conditions. The experimental materials were worn by a steel ball with ∅ 5 mm, loaded by 8 N. The sliding speed was 0.2 m/s, the sliding distance 360 m. Experiments were done in dry conditions and with lubricant (specimen and pin were underwater in ca 0.1 l - transmission oil Mogul SAE 80), the coefficient of friction as well as wear damage during whole test were measured and recorded.

RESULTS AND DISCUSSION

The basic mechanical properties of the two variants of the experimental material are determined by their microstructure resulting from the heat treatment and status of the surface [7]. The differences between the two variants are as follows:

Material A: AstCrM + 0.3C – sintering – case-hardening – hardening – tempering

Material B: AstCrM + 0.3 C – sintering – shoot peening – case-hardening - hardening – tempering

Tab.1. Properties of the experimental materials.

Mat.	Surface	Density [g·cm^{-3}]	Structure	Hardness HV	Depth of case hardened layer
A	Case hardening	~7.0	Temp. martensite + carbides	415	~ 700 μm
B	Case hardening + shoot peening approx. 60 μm	~ 6.95	Temp. martensite + carbides	485	~ 650 – 700 μm

The microstructure of the surface of the material A, Fig.2a, consists of tempered martensite and a network of coarse carbides (mostly probably M_3C) segregated along boundaries of pores. The material B is shown in Fig.2b. Here, a large amount of segregated fine carbides is observable in the surface layer, where the influence of shoot peening is evident.

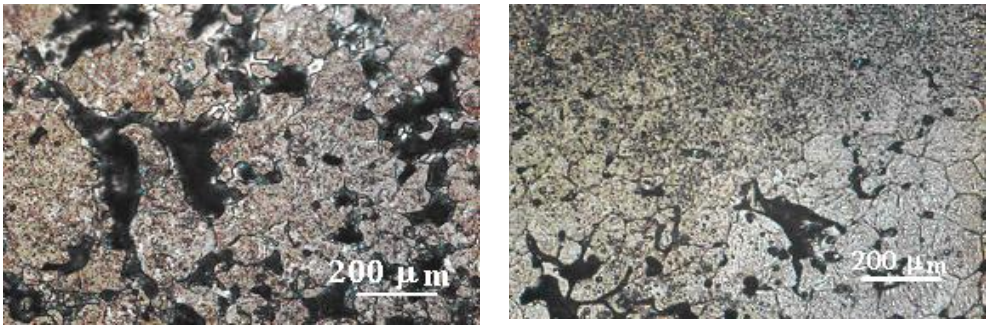

Fig.2a,b. Microstructure of the materials A and B following heat treatment by case hardening.

The results of the contact fatigue are in Fig.3. According to the graph, the service life of the case-hardened material was about $50 \cdot 10^6$ cycles for the load of 1790 MPa. The resistance of the material, which was before case-hardening treated by shoot peening, increased to 2920 MPa, a rise of about 63%, which can be attributed to two factors. Firstly, shoot peening the surface leads to its compaction, which meant an increase of the surface density from the original value of about 7 $g \cdot cm^{-3}$ up to approximately 7.4 – 7.5 $g \cdot cm^{-3}$. This increased the strength and hardness of the surface layer and introduced beneficial compressive stresses into it. Secondly, during case-hardening such material behaved differently from the more porous one. This difference is also evident from comparing Figs.2a and 2b.

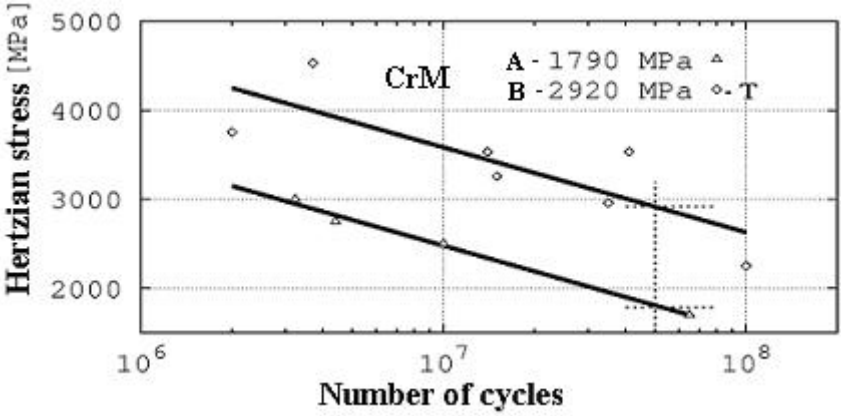

Fig.3. Fatigue curves after contact loading.

Contact fatigue damage causes the creation of pitting. In the material A, whose surface had not been previously treated and whose microstructure contained networks of

carbides, a gradual break out of particles occurred along the entire wear track, around which segregated carbide particles are located, Fig.4a. Since these broken out particles are smaller than a typical powder particle, the overall damage is thus a sum of smaller damages. In material B a pulling out of larger particles, in fact the original powder particles, took place. In this case the size of pitting corresponds to the size of the powder particle (approx. 150 μm). The surface compaction of the treated material also affected the damage mechanism.

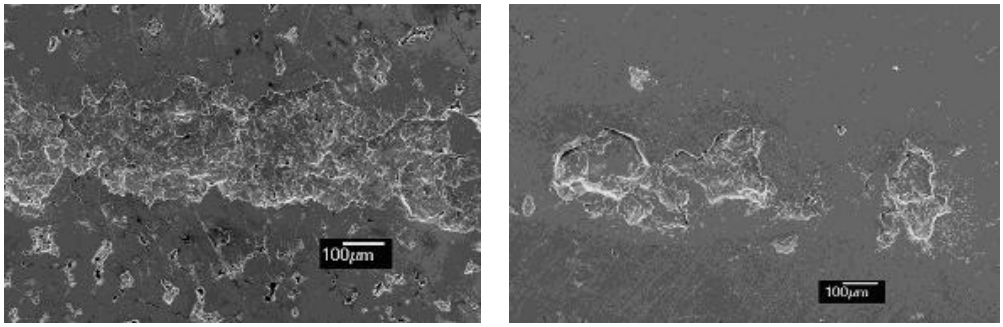

Fig.4. Pittings on investigated materials: a) material A, b) material B.

With respect to the size of the pulled out particles in the material A, mini-cracking, with mechanisms corresponding to ductile and brittle fracture, took place. In material B fractographic features typical for striation mechanism, Fig.5, typical for compact materials, could also be observed.

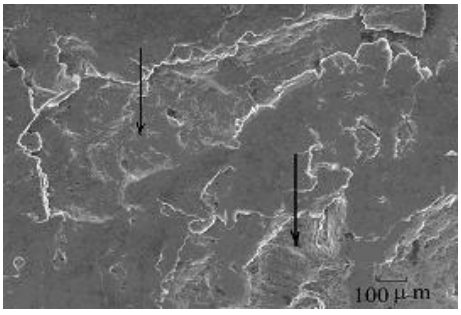

Fig.5. Striation inside the pitting sites.

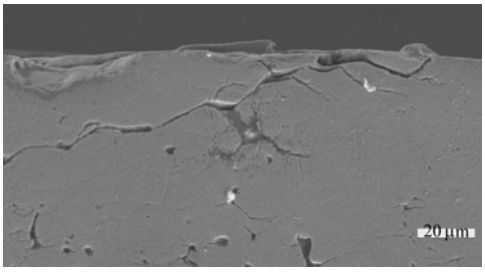

Fig.6. Cracks growing from the surface of material B.

This account is also supported by the appearance of a classical fracture (realized with impact load) in both materials, Figs.7,8. The cross sections of the pitting sites showed that cracks leading to pitting originated at the exposed surface in both materials. No crack initiation was found in the depth that corresponds to maxima of Hertzian stresses (range from 0.022 – to 0.093 mm by stresses from 1044 – to 4424 MPa), Fig.6.

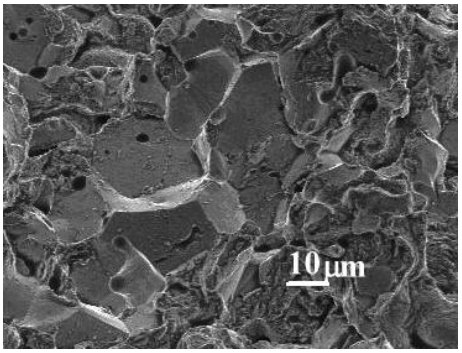

Fig.7. Fragile splitting facettes on non shot-peened surface.

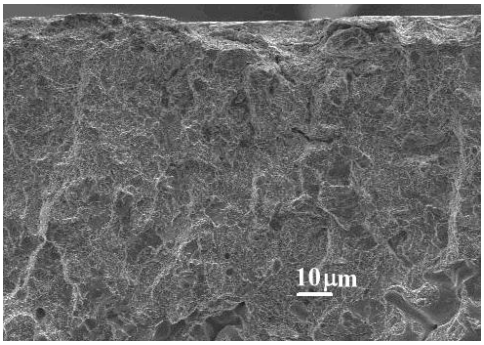

Fig.8. Ductile Fracture on shot- peened surface cross section.

Figures 9-10 show the results of tribological testing. In Fig.9 development of the friction coefficient with the sliding distance is shown. With lubricant, both materials had very low, almost identical friction coefficients. In dry conditions the results are very different. The material B, as expected, exhibited high friction during the entire test. On the other hand, material A had values of friction similar to those found in tests with lubricant.

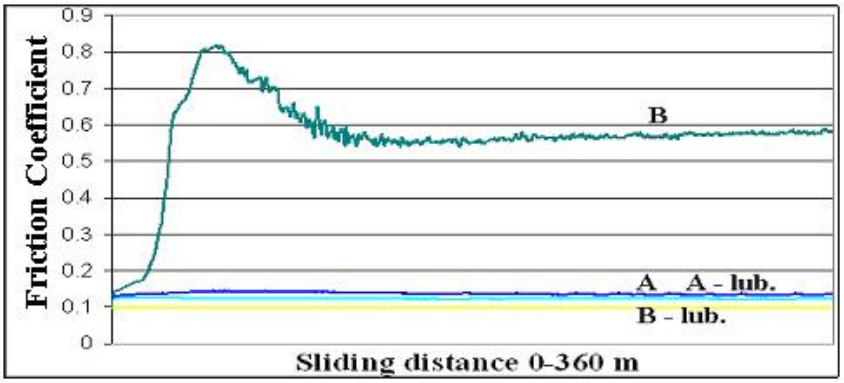

Fig.9. Coefficient of friction as a function of sliding distance.

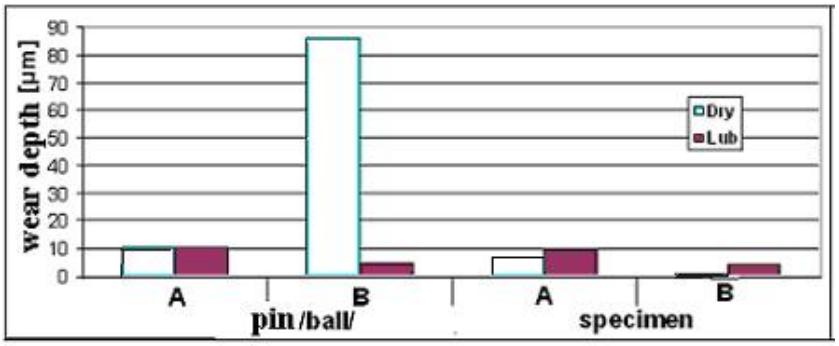

Fig.10. The overall wear on the distance dependence.

These values correspond well to the overall wear damage graph, as illustrated in Fig.10. This overall wear consists of the sum of wear of both the material and the pin (ball). Here one can see that for the test involving material B in dry conditions, higher wear was found but the damage is mostly the wear of the pin (ball), wear of the experimental material is minimal. This fact is in accordance with microscopic observations of both worn surfaces – material and pin, Figs.11-12.

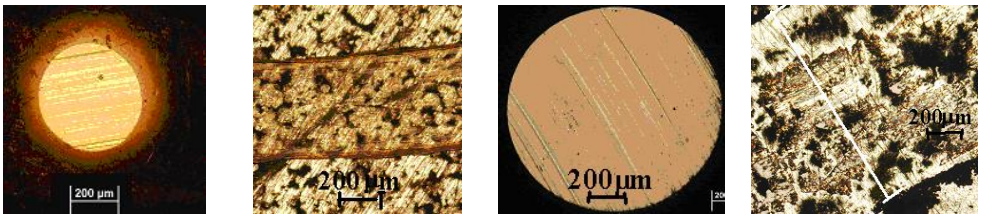

a b c d

Fig.11. Wear of the material A: a – indenter, b – sample; material B: c – indenter, d – sample; dry sliding.

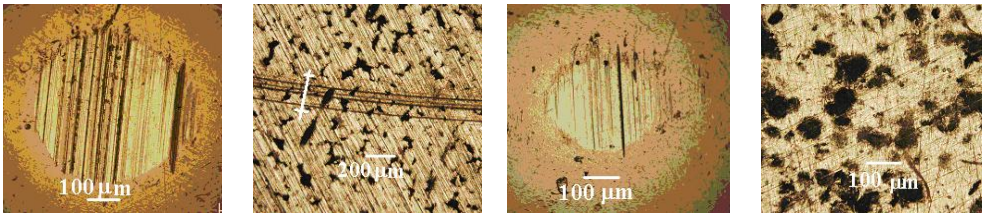

a b c d

Fig.12. Wear of the material A: a – indenter, b – sample; material B: c – indenter, d – sample; tested in lubricant.

High wear of the pin has its origin in microstructure. The surface is toughened, without pores and it contains fine carbides of high hardness. Against this surface is rubbed a material of lower hardness. The idea is similar to grinding metallic material with sand paper.

What caused such a low coefficient of friction in material A, the surface of which was not shoot peened before case-hardening, and correspondingly low wear damage of both the material and the pin, remains to be explained. The exact explanation of this phenomenon, found also in AstCrL [11], as well as other phenomena which appear to contradict expectations and results of other authors for PM materials, e.g. [4], is not available at the present state of research. There is not enough data to make a clear assertion. We lean towards the general opinion that the wear of the material A is fundamentally influenced by pores present on the surface [9, 10]. What are the exact mechanisms by which these pores work (one of the possible mechanisms assumes that pores act as a reservoir of worn material [8]) must be a subject of independent and carefully planned research activities.

CONCLUSIONS

1. Measured values of the contact fatigue resistance of the experimental materials showed a beneficial effect of case-hardening when compared to the as-sintered state, an increase from 1310 MPa up to 1790 MPa (results of contact fatigue testing for as-sintered materials without surface treatment will be published shortly).

2. The positive influence of case-hardening is even more evident when the material is treated beforehand by shoot peening, which improves surface quality. The fatigue limit grew from 1790 up to 2920 MPa.
3. In the treated surface layer, cracks grew not only by classical ductile / brittle mechanisms but also by fatigue striation.
4. The mechanism of surface damage is governed by pittings which originate in cracks initiated by surface pores. No cracks have been observed located in the sites of subsurface Hertzian stress maxima.
5. The results of tribological testing, especially those performed in lubricant (same environment as in the case of contact fatigue experiments) show no correlation with the contact fatigue results.
6. The results of dry sliding correspond to the phenomena originated on the interface as a result of the specific properties of both surfaces (material and pin).

Acknowledgements

The work was supported by common projects of the Ministry of Education and Slovak Academy of Sciences VEGA 1/0464/08 and VEGA 2/0120/10. The tribological testing was carried out within the framework of the project „Centre of Excellence of Advanced Materials with Nano- and Submicron Structure“, which is supported by the Operational Program “Research and Development” financed through European Regional Development Fund.

REFERENCES

[1] Lipp, K., Sonsino, CM., Pohl, D., Hock, S. In: Procceding of the 1998 Powder Metallurgy World Congress and Exhibition. Vol. 3. Granada, Spain. Shrewsbury : EPMA, p. 143
[2] Lipp, K., Sonsino, CM., Pohl, D., Brandt, W. In: PM '94 Powder Metallurgy World Congress. Vol. 2. Paris. Societe Francaise de Metallurgie et de Materiaux, Les Editions de Physique, 1994, p. 831
[3] Forden, L., Bengtsson, S., Lipp, K., Sonsino, CM. In: Procceding of the 2003 EURO PM Congress. Vol. 3. Granada, Spain. Shrewsbury : EPMA, p. 143
[4] Alzati, L., Engström, U., Rivolta, B., Tavasci, A. In: Proceedings of the 2008 World Congress on Powder Metallurgy & Particulate Materials. Washington, USA, Part 10, 2008, p. 1
[5] Bengtsson, S., Marcu, T., Klekovkin, A. In: Proceedings of the 2008 World Congress on Powder Metallurgy & Particulate Materials. Washington, USA, Part 6, 2008, p. 1
[6] Engström, U., Milligan, D., Klekovkin, A., Berg, S., Edwards, B., Fryman, L., Hinzmann, G., Whitehouse, D. In: International Conference on Powder Metallurgy & Particulate Materials. Part 10. Montreal, Canada. Princeton : MPIF, 2005, p. 170
[7] Čajková, L.: Pevnosť a húževnatosť moderných vysokopevných spekaných ocelí. Dizertačná práca. Košice : ÚMV SAV, 2007 (in Slovak)
[8] Simchi, A., Danninger, H.: Powder metall., vol. 47, no. 1, p. 73
[9] Bidulský, R., Actis-Grande, M.: High Temperature Materials and Processes, vol. 27, 2008, no. 4, p. 249
[10] Khorsand, H., Habibi, SM., Yoozbashizadea, H., Janghorban, K., Reihani, SMS., Rahmani Seraji, H., Ashtari, M.: Materials and Design, vol. 23, 2002, p. 667
[11] Babakhani, A., Haerian, A., Ghambri, M.: Journal of Mat. Proces. Technol., vol. 204, 2008, p. 192
[12] Rodziňák, D., Semrád, K., Hvizdoš, P., Zahradníček, R., Zahradníček, V. In: 10th International Symposium Intertribo 2009. Vysoké Tatry - Stará Lesná, 2009, p. 13